Seasonal and Synoptic Variations in Near-Surface Air Temperature Lapse Rates in a Mountainous Basin

TROY R. BLANDFORD, KAREN S. HUMES, BRIAN J. HARSHBURGER, BRANDON C. MOORE, AND VON P. WALDEN

Department of Geography, University of Idaho, Moscow, Idaho

HENGCHUN YE

Department of Geography and Urban Analysis, California State University, Los Angeles, Los Angeles, California

(Manuscript received 29 August 2006, in final form 14 March 2007)

ABSTRACT

To accurately estimate near-surface (2 m) air temperatures in a mountainous region for hydrologic prediction models and other investigations of environmental processes, the authors evaluated daily and seasonal variations (with the consideration of different weather types) of surface air temperature lapse rates at a spatial scale of 10 000 km^2 in south-central Idaho. Near-surface air temperature data (T_{max}, T_{min}, and T_{avg}) from 14 meteorological stations were used to compute daily lapse rates from January 1989 to December 2004 for a medium-elevation study area in south-central Idaho. Daily lapse rates were grouped by month, synoptic weather type, and a combination of both (seasonal–synoptic). Daily air temperature lapse rates show high variability at both daily and seasonal time scales. Daily T_{max} lapse rates show a distinct seasonal trend, with steeper lapse rates (greater decrease in temperature with height) occurring in summer and shallower rates (lesser decrease in temperature with height) occurring in winter. Daily T_{min} and T_{avg} lapse rates are more variable and tend to be steepest in spring and shallowest in midsummer. Different synoptic weather types also influence lapse rates, although differences are tenuous. In general, warmer air masses tend to be associated with steeper lapse rates for maximum temperature, and drier air masses have shallower lapse rates for minimum temperature. The largest diurnal range is produced by dry tropical conditions (clear skies, high solar input). Cross-validation results indicate that the commonly used environmental lapse rate [typically assumed to be -0.65°C (100 m)$^{-1}$] is solely applicable to maximum temperature and often grossly overestimates T_{min} and T_{avg} lapse rates. Regional lapse rates perform better than the environmental lapse rate for T_{min} and T_{avg}, although for some months rates can be predicted more accurately by using monthly lapse rates. Lapse rates computed for different months, synoptic types, and seasonal–synoptic categories all perform similarly. Therefore, the use of monthly lapse rates is recommended as a practical combination of effective performance and ease of implementation.

1. Introduction

Surface air temperature is a controlling factor of many environmental processes. Therefore, it is important to many fields of research, including hydrology (Blöschl 1991; De Scally 1997; Richard and Gratton 2001; Zuzel and Cox 1975), glaciology (Singh and Singh 2001), ecology (Lechowicz 1984; Peacock 1975; Stoutjesdijk and Barkman 1992), and agricultural and natural resource management (Bibby et al. 1982; Régnière and Bolstad 1994). Accurate spatially distributed estimates of surface air temperature are critical to many hydrological (Ferguson 1999; Martinec and Rango 1998; Wigmosta et al. 1994) and ecological models (Thornton et al. 1997). Additionally, the field of weather forecasting has much to gain from research regarding the spatial behavior of near-surface air temperature. Gridded graphical forecasts developed over the past few years by the National Weather Service are a good example of how lapse rates are being applied to coarse model grids in order to generate more realistic temperature distributions in mountainous terrain (Glahn and Ruth 2003).

Linear lapse rates are commonly used in hydrologic

Corresponding author address: Troy Blandford, Department of Geography, University of Idaho, Moscow, ID 83844.
E-mail: troy.blandford@uidaho.edu

DOI: 10.1175/2007JAMC1565.1

and terrestrial models to interpolate near-surface air temperature measurements from meteorological stations to locations at different elevations where measurements do not exist (Martinec and Rango 1998; Régnière 1996; Running et al. 1987; Thornton et al. 1997). The commonly used average environmental lapse rate of $-0.65°C\ (100\ m)^{-1}$ (Barry and Chorely 1987) is a spatially global and temporally climatic average (or standard); it should be applied with caution at other scales (e.g., changes with latitude; De Scally 1997; Tabony 1985). Its use may be particularly problematic at short temporal and fine spatial scales because lapse rates show significant variability (De Scally 1997; Dodson and Marks 1997; Pepin et al. 1999; Rolland 2003). This variability should be accounted for when using lapse rates to extrapolate air temperature.

A distinction should be made between free-air lapse rates and near-surface lapse rates (Harlow et al. 2004; McCutchan 1983; Pepin et al. 2005; Richner and Phillips 1984). Because they are impacted by different processes, near-surface and free-air lapse rates may be very different at a given time and place. This is an especially important distinction to make in mountainous regions where the "heated" land surface is essentially projected (in the form of mountains) into the free air. Near-surface lapse rates are more variable than free-air lapse rates (Harlow et al. 2004). This analysis is concerned with near-surface lapse rates.

Near-surface temperatures typically decrease with increasing elevation. However, under certain conditions the opposite effect may occur. The influences of inversion, insolation, katabatic wind, and cold air drainage on the air temperature gradient in mountainous basins, especially on minimum temperature, are well documented (Barry 1992; Clements et al. 2003; Mahrt et al. 2001; Whiteman et al. 1999).

Near-surface lapse rates vary diurnally and seasonally. Pepin et al. (1999) and Rolland (2003) investigated lapse rate variations in the Pennines of northern England and throughout the Italian and Austrian Alps, respectively. Lapse rates were generally steeper (greater decrease in temperature with height) during the day than at night and during warmer months than colder months. Increased inversion frequency during colder months partially explains the seasonal trend in lapse rates (Whiteman et al. 1999).

Several studies have investigated the impacts of synoptic weather conditions, or large-scale weather patterns, on lapse rates (Pepin et al. 1999; Stahl et al. 2005). Pepin et al. (1999) conducted a study in the uplands of northern England evaluating the relationships between lapse rates and solar radiation, humidity, wind speed, and synoptic types. Steeper lapse rates occurred with higher levels of solar radiation. At night, wind speed also steepened the lapse rates, but during the day this relationship was weak. At high wind speeds ($>5\ m\ s^{-1}$), the near-surface lapse rate tended to converge toward the dry adiabatic lapse rate $[-0.98°C\ (100\ m)^{-1}]$. Anticyclones, typically associated with clear, calm weather, tended to increase the magnitude of the diurnal lapse rate cycle. Daytime lapse rates were steep under anticyclonic conditions because of increased solar radiation receipt, and nocturnal lapse rates were shallow (lesser decrease in temperature with height) because of higher inversion frequencies during cloud-free nights. Moister atmospheres produced shallower lapse rates. Lapse rates during humid conditions approximated the moist adiabatic lapse rate [usually near $-0.40°C\ (100\ m)^{-1}$]. Southerly airflow also produced shallower lapse rates because of the advection of warmer air into higher elevations, thereby decreasing the temperature–elevation (T–E) relationship. In contrast to Pepin et al. (1999), Stahl et al. (2005) found that the steepest lapse rates in British Columbia, Canada, were associated with a low pressure system characterized by strong westerly to southwesterly winds and high amounts of precipitation. Clearly, the impacts of synoptic weather types on lapse rates vary by season and by location.

The objective of this work is to quantify seasonal and synoptic variations in near-surface air temperature lapse rates. As described previously, Pepin et al. (1999), Rolland (2003), and Stahl et al. (2005) have investigated these aspects of lapse rates before, but primarily at regional scales. Many ecologic and hydrologic modeling efforts require spatial interpolation of air temperature at the scale of smaller basins. One factor that has limited past examinations of lapse rates at landscape scale is the relatively small number of meteorological stations typically available in mountainous watersheds. However, with the advent and recent expansion of the Natural Resources Conservation Service (NRCS) snowpack telemetry (SNOTEL) network, there are now an increasing number of stations with a long enough data record that are suitable for analysis.

The new elements of work presented here include the following: (i) lapse rates are evaluated at a landscape scale ($<10\ 000\ km^2$) and, therefore, represent local phenomena; and (ii) errors incurred using the standard environmental lapse rate [ELR, assumed to be $-0.65°C\ (100\ m)^{-1}$] and a locally computed regional lapse rate are compared through cross-validation with errors incurred using monthly and synoptic mean lapse rates.

2. Study area

The study area is located in south-central Idaho, near Boise, at approximately 43°52′N, 115°15′W (Fig. 1).

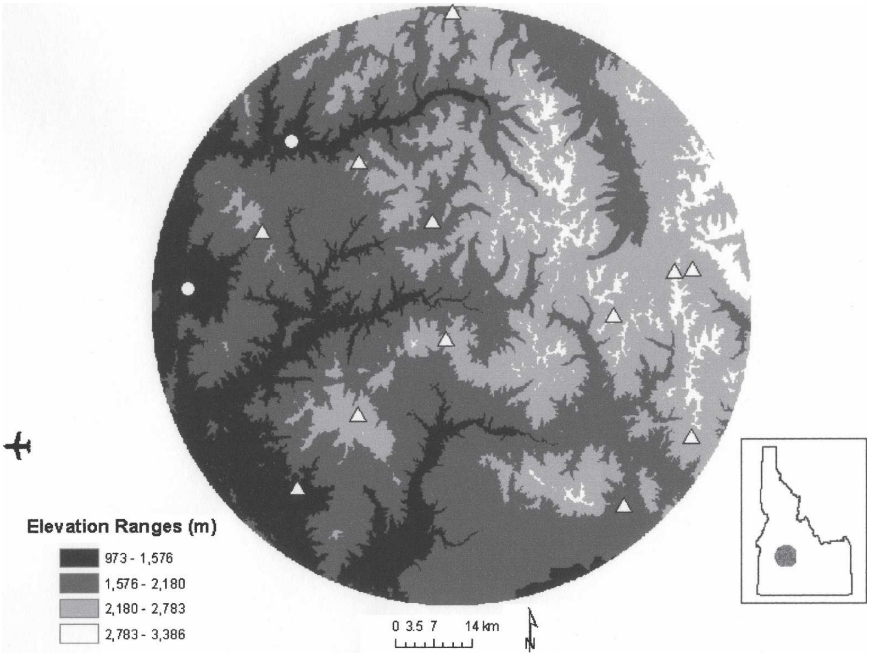

FIG. 1. Topography and the locations of 14 meteorological observation stations near Boise, ID. Triangles represent SNOTEL stations; circles represent COOP stations. The study area encompasses approximately 10 000 km^2. The airplane symbol west of the basin represents the Boise airport, where synoptic weather types are provided by the Spatial Synoptic Classification system (Sheridan 2002).

The area is circular because a ½°-radius search ellipse was used to identify meteorological stations to use in the study. This ensured that all stations were within 1° of each other, which was suggested by Rolland (2003) as the largest spatial extent over which lapse rates should be expected to remain consistent. Assuming a stationary lapse rate beyond this spatial extent is questionable. The circle encompasses an area of approximately 10 000 km^2. This is a smaller spatial extent than other daily air temperature spatial interpolation studies [e.g., 830 000 km^2 for Dodson and Marks (1997), 260 000 km^2 for Harlow et al. (2004), and 400 000 km^2 for Thornton et al. (1997)].

The study area ranges in elevation from 970 m in the west to 3390 m in the east (relief of ~2400 m). The region is typical of much of the central and northern portions of the Rocky Mountain region with wet winters and dry summers. Annual normal temperature ranges from 5°C in higher elevations to 16°C in lower elevations. The study area is practical for developing and testing techniques for generating daily spatial fields of temperature in small, mountainous regions, because it contains enough meteorological stations that developing temperature–elevation regressions is feasible, but not so many that it is atypical of station density in other areas of the Pacific Northwest.

The spatial locations of 14 surface observation sites are shown in Fig. 1. The station elevations (Fig. 2) are representative of the elevation range (asterisks) in the study area. Stations are distributed across the region with a range of slope, aspect, and land-cover characteristics (Table 1). A multiple linear regression analysis of the station temperature observations and various land characteristics indicated that, besides elevation, other variables (slope, northness, land cover, distance east, distance north, terrain ruggedness, and station height above the local minimum) showed minor influences on station temperatures. That is, once the elevation trend was removed from the temperature values, additional covariables explained only small amounts of the remaining variance. Therefore, in our study area, differences in the landscape characteristics of the stations do not seem to significantly influence the observed temperatures. This is possibly due to the small spatial extent of the study area and to stations traditionally being placed on relatively flat, open sites away from tall vegetation.

3. Methods

a. Station selection and data preparation

Meteorological station data were obtained from the National Weather Service's Cooperative Observer Program (NWS COOP) and the NRCS SNOTEL network.

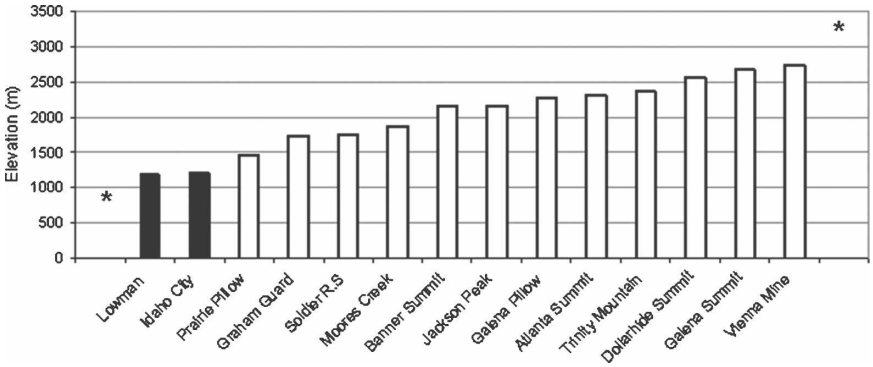

FIG. 2. The elevations of stations used in the analysis. White bars represent SNOTEL stations; black bars represent COOP stations. Asterisks mark the lowest and highest elevations in the study area.

NWS COOP data were obtained via the Internet from the National Climatic Data Center (http://cdo.ncdc.noaa.gov/CDO/cdo). NRCS SNOTEL data were obtained from the National Water and Climate Center (http://www.wcc.nrcs.usda.gov/snotel). Daily values of near-surface (2 m) air temperature maximum (T_{max}) and minimum (T_{min}) were available from these sources. Although observation times are different for SNOTEL (midnight) and COOP stations [early morning, 0800 mountain standard time/mountain daylight time (MST/MDT), or late evening, 1700 MST/MDT], recordings are assumed to represent the same previous 24 h. On some days COOP stations may have bias extreme temperature observations because they are made at certain times of the day (rather than midnight to midnight). Such days are assumed to be rare enough as to not affect the overall results of this study.

Average temperature (T_{avg}) was computed as the mean of T_{max} and T_{min}. An analysis of 30 days of data selected at random from SNOTEL stations in the study area indicated that the averaging of T_{max} and T_{min} is typically within 1°C of the average daily temperature computed using 3-h data. The simple average of T_{max} and T_{min} was therefore used in order that T_{avg} could be computed consistently for all stations in the analysis.

Meteorological stations were selected based on three criteria: 1) stations located within ½° radius of the center of the study area were used; 2) stations needed to have a period of record that matched the period of record of the other stations; and 3) stations could not have more than 15% missing data after quality control.

Quality control was performed following techniques described by Reek et al. (1992). Three primary checks were performed: 1) maximum temperature must be greater than minimum temperature; 2) temperature values should not exceed the historically recorded minimum or maximum for Idaho (−51°, 48°C); and 3) values should not be the same (to the 10th) for three or more consecutive days ("flatliner" phenomena; Reek et al. 1992). Any suspicious data were flagged with the

TABLE 1. List of the weather stations used in this analysis, including elevation and topographic characteristics.

Station name	Elev (m)	Easting (m)	Northing (m)	Slope or valley	Aspect	Land cover
Lowman	1195	371 601.64	332 488.38	Valley	South (flat)	Shrubland
Idaho City	1209	352 517.24	305 279.47	Valley	East	Urban
Prairie Pillow	1463	372 836.12	268 340.09	Valley	South (flat)	Urban
Graham Guard	1734	397 809.00	317 792.57	Valley	East	Grassland
Soldier R. S. Pillow	1750	433 191.75	265 112.71	Valley	East	Shrub (riparian)
Moores Creek	1859	366 287.31	315 905.08	Slope	West (?)	Conifer forest
Banner Summit	2146	401 529.10	356 539.20	Slope	North	Conifer forest
Jackson Peak	2155	384 362.96	328 762.89	Slope	North (?)	Conifer forest
Galena Pillow	2268	445 974.14	308 675.95	Valley	East	Conifer forest
Atlanta Summit	2310	400 265.44	295 808.74	Slope	North	Conifer forest
Trinity Mountain	2368	383 972.47	281 908.75	Slope	North	Conifer forest
Dollarhide Summit	2566	445 756.07	277 852.11	Slope	East	Deciduous forest
Galena Summit	2676	442 665.98	308 435.54	Slope	West	Conifer forest
Vienna Mine	2731	431 407.36	300 163.87	Slope	West	Conifer forest

value −9999 and confirmed manually before deletion from the dataset.

The aforementioned selection criteria resulted in 14 meteorological stations (2 NWS COOP and 12 NRCS SNOTEL) with an overlapping period of record from 1 January 1989 to 31 December 2004 (station locations shown in Fig. 1). A day was removed from the entire dataset only if more than one station was missing data for that day. This maximized the number of days available to compute *T–E* regressions while ensuring that they were consistently computed with at least 90% of the stations (13 or 14). Days that did not have a synoptic classification (discussed later) also had to be removed. Of the 5844 days between 1 January 1989 and 31 December 2004, approximately 5% were removed. This resulted in a working dataset of 5527 days.

b. Synoptic classification

Synoptic conditions, or general weather types, may explain day-to-day variations in lapse rates (Pepin et al. 1999; Stahl et al. 2005). Many classification methods ranging from manual and subjective to automated and objective have been developed (Jones et al. 1993; Kidson 1994; Lamb 1972; Mayes 1991; Muller 1977; Schwartz 1991). The Spatial Synoptic Classification (SSC2) system was used in this research (Sheridan 2002) because it is spatially transferable and has a long period of record available for Boise, Idaho.

The SSC2 is spatially transferable, and its classification scheme is relative to each particular geographic location (i.e., a dry moderate classification in Texas is different than dry moderate in Idaho). Likewise, dry moderate conditions are cooler in winter than in summer at all locations. Seed days (days that typify a weather type) are identified from a historical record at each station and allow the classification to concern itself with local meteorological character (Sheridan 2002). This was valuable to this analysis because it allowed the determination of a local lapse rate response to the weather type. The SSC2 was also chosen because a historic record (1948 to 2005) of day-by-day weather types is readily available (http://sheridan.geog.kent.edu/ssc.html).

The weather conditions for each day are categorized into six different types, or as transition between two types. The weather types are 1) dry moderate (DM), 2) dry polar (DP), 3) dry tropical (DT), 4) moist moderate (MM), 5) moist polar (MP), and 6) moist tropical (MT).

Because these weather conditions are fashioned to a particular station, they are described below primarily in relevance to the Boise, Idaho, airport weather station (SSC2 code BOI), located approximately 30 km west of the study area (airplane symbol in Fig. 1). Although the SSC2 classification is not provided directly in the study area, synoptic conditions a short distance to the east are assumed to be similar, because weather patterns in the area typically traverse west to east, and "synoptics" by definition capture large-scale, general conditions.

DM conditions are typified by mild and dry air. Zonal flow aloft is common during DM conditions and allows the air to dry and warm adiabatically, which may produce a steeper *T–E* gradient than normal.

DP conditions are typified by cool or cold, dry air originating in Canada or Alaska. Northerly winds are common and cloud cover is minimal. Inversions may set up for extended periods during DP as the cold air sinks and displaces warmer air, especially at night.

DT weather is hot, dry, and sunny. It is typically pushed into Idaho from the southwest. Violent downslope winds may also produce DT conditions. Because of the extreme heat and associated dryness the *T–E* gradient may approach the dry adiabatic lapse rate [-0.98°C (100 m)$^{-1}$].

MM conditions are cloudy, warm, and humid. They are common during mild winters and may persist for many days. MP conditions are similar to MM but are cooler and less humid. Light precipitation is common. MP conditions are common during winter in Idaho, as is typical of a Mediterranean climate.

MT weather occurred only 2.3% of the days at the Boise station and was, therefore, not used in the analysis. The frequency of occurrence of the other weather types is shown in Fig. 3 and summarized by month in Fig. 4. DM conditions occur most frequently except in summer, and are common during all months. In general, relatively dry conditions (DM, DP, and DT) dominate the study area for nine months of the year.

c. Computing T–E regressions and comparing group means

Near-surface lapse rates were estimated from observed temperature (2 m) data using linear regression [Eq. (1)], where elevation is the independent variable and air temperature is the dependent variable (Harlow et al. 2004; Rolland 2003). From here forward, the near-surface lapse rate will be used synonymously with "*T–E* relationship," or "regression," to signify how it is computed:

$$T_{\mathrm{obs},j} = \beta_1 h_j + t_0, \tag{1}$$

where $T_{\mathrm{obs},j}$ is the observed air temperature (°C) at station j, β_1 is the slope coefficient/lapse rate (°C m^{-1}), h_j is the latitude (m) at station j, and t_0 is the temperature (°C) at sea level (0 m, y intercept).

T–E regressions were computed on a daily basis and then grouped by month, synoptic type, and a combina-

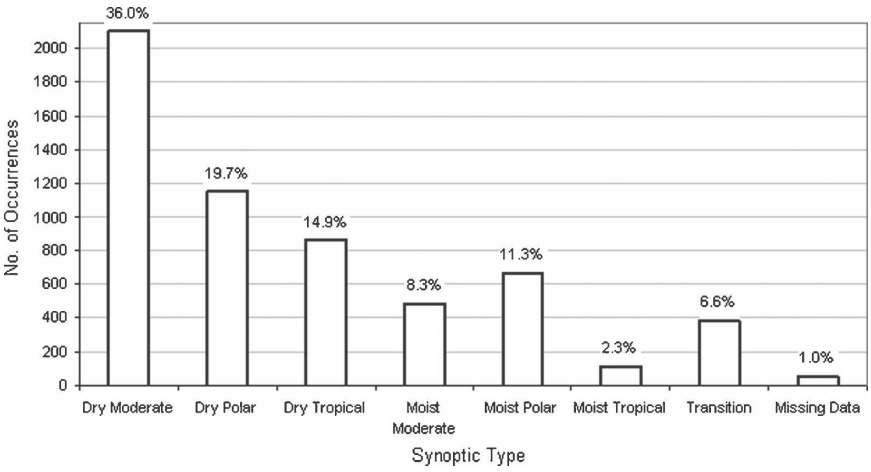

FIG. 3. The number of occurrences of synoptic weather types in the study area from 1 Jan 1989 to 31 Dec 2004. The frequency of occurrence of each synoptic weather types is shown above each bar.

tion of these two groupings (seasonal–synoptic). The seasonal–synoptic groups were created using four seasons (December–February, March–May, June–August, and September–November) and the synoptic groups that occurred within them. There were 12 month groups, 6 synoptic groups, and 24 seasonal–synoptic groups. Although the sample sizes of the month groups were all relatively the same, the sizes of the other groups varied, as described by the frequency histograms in Figs. 3 and 4.

Student's t test of difference in mean, which takes different sample sizes into account, and one-way analysis of variance (ANOVA) were then used to compare the population means of different groups. First, a one-sample t test was performed to determine if group means were statistically different from the average atmospheric lapse rate [$-0.65°C\ (100\ m)^{-1}$]. A second one-sample t test was then performed to determine if the mean of each group was different from a regional lapse rate (an average lapse rate computed from all 5527 days, i.e., the mean of the total population). Third, one-way ANOVA was used to compare one group to each of the others, iteratively. These three steps respectively determined (a) if a lapse rate other than the average atmospheric lapse rate was necessary for the study area; (b) if a lapse rate other than a regional lapse rate was necessary; and (c) if divisions amongst different groups were necessary.

One-way ANOVA essentially extends the two-sample t test (which compares the equality of two population means) to compare more than two means. It is equivalent to a t test when only two groups are compared. Since many groups were being analyzed, ANOVA was preferable in terms of efficiency. For example, instead of performing numerous t tests (e.g., January versus February, January versus March, Janu-

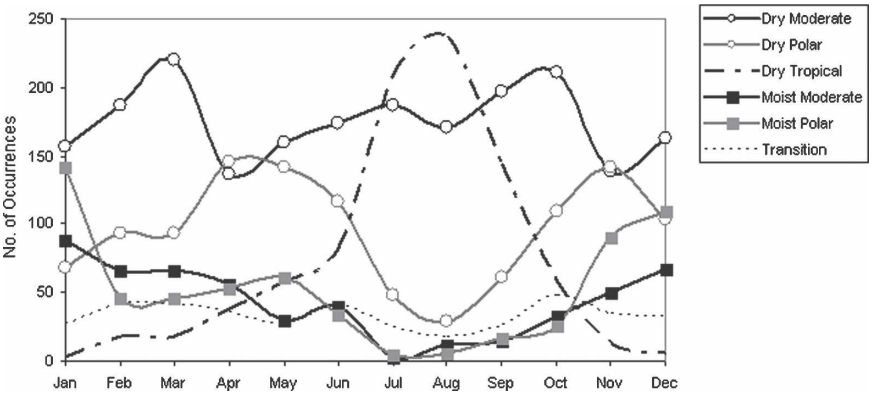

FIG. 4. The number of occurrences of synoptic weather types in the study area by month.

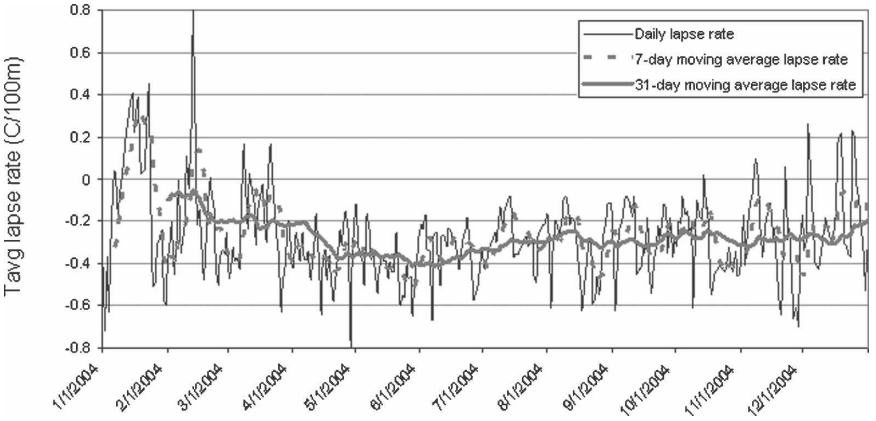

FIG. 5. The daily variation of T_{avg} lapse rates. The 7- and 30-day running averages are also shown. The *T–E* regression resulting in the extreme inversion value [+0.80°C (100 m)$^{-1}$] seen in mid-February had a strong fit (r^2 = 0.80), and is therefore not suspected to be in error.

ary versus May) all of the months were analyzed against each other at once. This was done in a two-step process.

First, one-way ANOVA was used to test whether or not all of the groups were equivalent based on an F statistic. This initial test indicated only that differences existed among the group means; it did not indicate which groups were different. Therefore, a post hoc test was necessary to make multiple comparisons. Using confidence intervals (alpha = 0.05) set on the difference between group means, the post hoc comparison identified which groups were significantly different from each other.

d. Cross-validation

To evaluate how well the group mean lapse rates predicted daily observed lapse rates, a cross-validation was performed. Each of the 16 yr was left out successively. The remaining data were grouped as before and the mean lapse rates were computed (predicted lapse rate dataset). Daily lapse rates for the year that was left out also were computed (observed lapse rate dataset) and then compared with the predicted lapse rate dataset. Results were summarized with mean error (ME; a bias indicator), mean absolute error (MAE), and RMSE (all in units of degrees Celsius per 100 meters).

4. Results and discussion

a. Daily lapse rate variation

As shown by the time series in Fig. 5, daily T_{avg} air temperature lapse rates showed high variability [standard deviation = 0.22°C (100 m)$^{-1}$] within a given year. Errors in the temperature observations may explain some of this variation; however, 7-day (dashed gray line) and 30-day (solid gray line) running averages, which smooth out much of this error, also show high variability (Fig. 5). Additionally, because the daily *T–E* linear regressions showed strong measures of goodness-of-fit (average r^2 = 0.6, and RMSE = 1.3°C), the scatter in the time series is primarily reflecting real phenomena in day-to-day lapse rate behavior, as opposed to reflecting errors in the temperature observations and analysis.

Daily T_{max} lapse rate variation (not shown) was lower than T_{avg} variability; T_{min} variation was higher. High variability in the daily lapse rates indicates that the ELR and regional lapse rate (RL) may perform poorly when used at subannual time scales.

b. Seasonal variations

Monthly values for T_{max} lapse rates have a distinct seasonal trend (Fig. 6a). Steeper lapse rates occurred during warmer months, while shallower lapse rates occurred during colder months. These findings are consistent with other literature (Harding 1979; Rolland 2003).

Mean T_{min} lapse rates are significantly shallower than mean T_{max} lapse rates for all months (Fig. 6b). They are also more variable, with a range from +0.03°C (100 m)$^{-1}$ in August and September to −0.36°C (100 m)$^{-1}$ in April. The distinct, gradual seasonal pattern observed in mean T_{max} lapse rates is not observed in T_{min} lapse rates. Instead, a general sinusoidal pattern emerges (steeper T_{min} lapse rates in spring, shallower lapse rates in late summer and early fall). This pattern is consistent with nighttime inversions, which frequently occur at night following warm, clear-sky days in summer and autumn. During warm months (July–Sep-

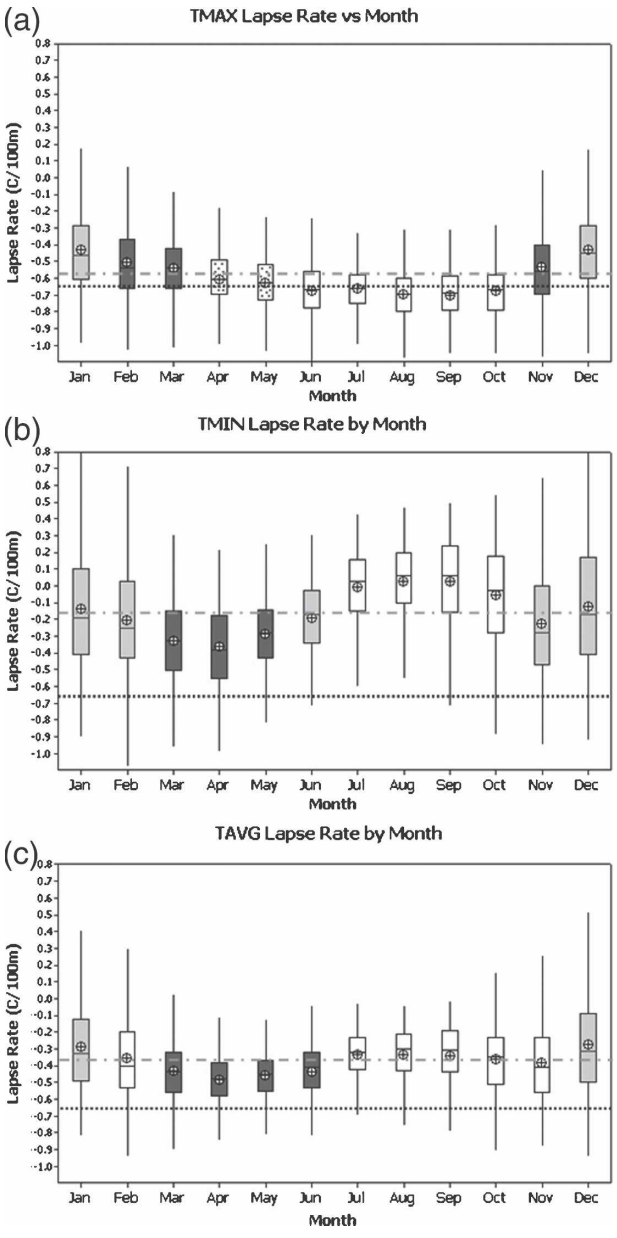

FIG. 6. Seasonal variations in lapse rates for (a) T_{max}, (b) T_{min}, and (c) T_{avg}. Dotted line represents the constant average environmental lapse rate; dot–dashed gray line represents the computed regional lapse rate. Shading shows box plots with statistically similar means.

tember), the box plots show an extremely shallow mean T_{min} lapse rate (even positive in August and September). Steeper T_{min} lapse rates did occur in August and September, as indicated by the extent of the box plot whiskers; however, extremely shallow or positive lapse rates are the norm (~60% of the study days). Daily T_{min} lapse rates from July to September equal or exceed the ELR (dotted black line) just 0.01% of the days. Daily T_{min} lapse rates are difficult to predict in winter—any mean lapse rate is a grossly smooth predictor.

As would be expected, T_{avg} lapse rates vary more than T_{max} and less than T_{min} lapse rates (Fig. 6c); T_{avg} lapse rates are shallowest in January and December [$-0.28°C\ (100\ m)^{-1}$] and steepest in April [$-0.49°C\ (100\ m)^{-1}$]. Additionally, cold months (November–February) are noticeably more variable than warmer months (May–August), as indicated by the bowtie-like pattern of the box plot whiskers. The seasonal trend seen in T_{max} lapse rates is not observed in T_{avg} lapse rates; instead, the pattern seen in T_{min} is prevalent, albeit more gradual.

c. *Variations by synoptic weather type*

Differences between T_{max} lapse rates for different synoptic categories are tenuous (Fig. 7a). Box plots for each synoptic category largely overlap. Dry moderate and moist moderate conditions have statistically identical means, as do dry polar and moist polar (shown by similar shading in the box plots). This is surprising considering relative moisture levels (dry versus moist) are expected to impact lapse rates. For example, Pepin et al. (1999) found significant positive correlations between lapse rates and humidity. Our study suggests that airmass temperature (polar versus moderate) impacts T_{max} lapse rates more than humidity level. This is further indicated by the stark difference between box plots for dry polar and dry tropical conditions.

Dry tropical conditions produced mean lapse rates that are significantly steeper than all other categories, except the "transition" category. Predictably, the transitional category results in a lapse rate statistically identical to the ELR, because both represent a wide range of conditions. During the summer, when dry tropical conditions are most common, strong surface heating causes the atmosphere to mix vertically through convection and leads to a dry adiabatic lapse rate (Pepin et al. 1999).

In contrast to T_{max}, dry tropical conditions result in a shallow, even slightly positive [$0.09°C\ (100\ m)^{-1}$], mean value for T_{min} (Fig. 7b). Cold air drainage likely occurs at night during clear sky (DT) conditions (Gustavsson et al. 1998). Also, unlike T_{max}, box plots for T_{min} show a difference between dry and moist air masses. This is especially shown by differences between dry moderate and moist moderate conditions. Box plots for DM conditions indicate markedly shallower rates than do the box plots for MM conditions, possibly due to the insolating effects of clouds observed during MM conditions. In general, steeper lapse rates occur during wetter con-

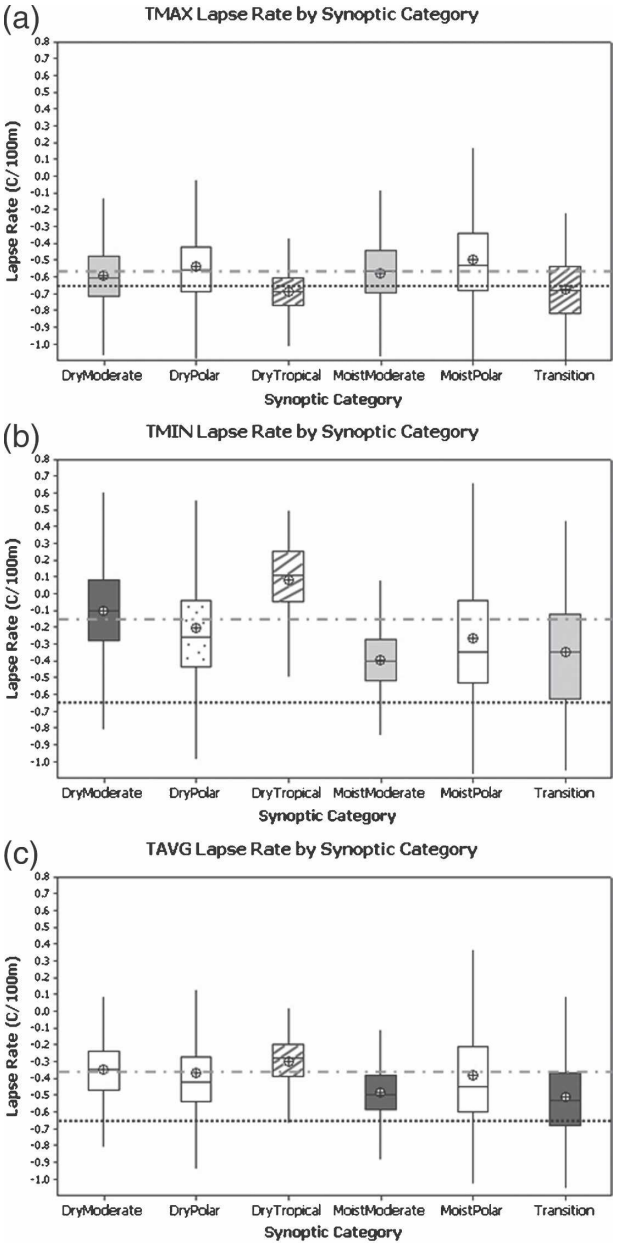

FIG. 7. Lapse rate variation by synoptic weather type for (a) T_{max}, (b) T_{min}, and (c) T_{avg}. Dotted line represents the average atmospheric lapse rate constant; dot–dashed gray line represents the computed regional lapse rate. Shading shows box plots with statistically similar means.

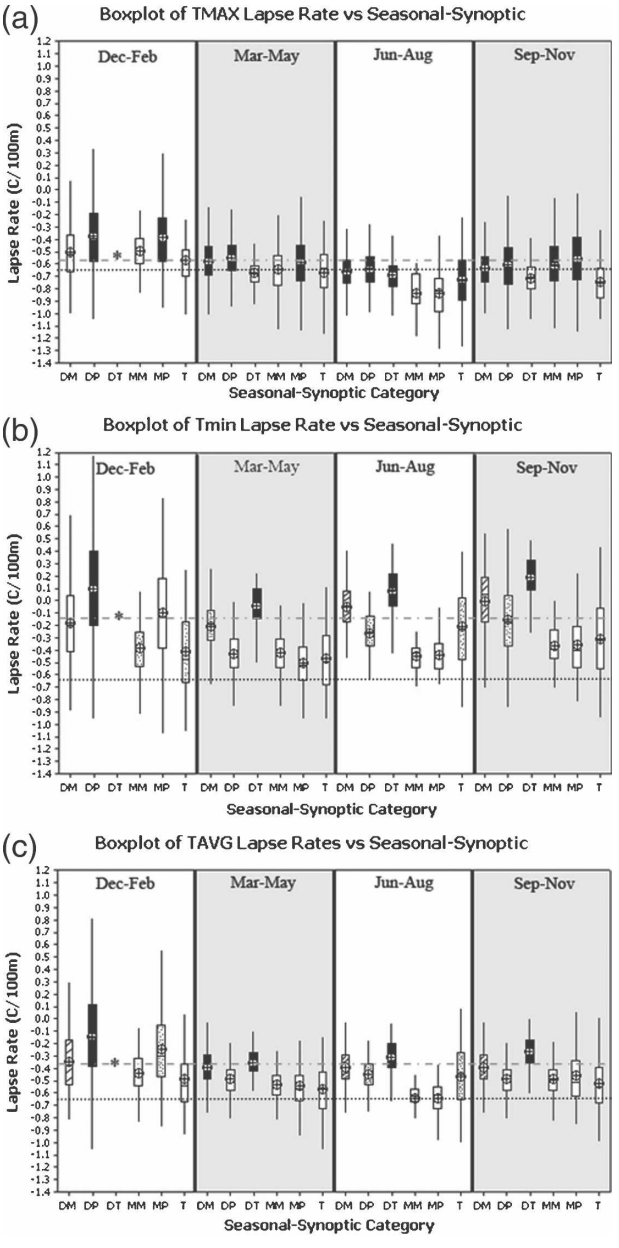

FIG. 8. Lapse rate variation by seasonal–synoptic groupings for (a) T_{max}, (b) T_{min}, and (c) T_{avg}. Dotted line represents the average environmental lapse rate constant; dot–dashed gray line represents the computed regional lapse rate. The asterisk in December–February notes a low sample size (n = 13) for DT. Shading shows box plots with statistically similar means (DM = dry moderate; DP = dry polar; DT = dry tropical; MM = moist moderate; MP = moist polar; T = transition).

ditions, while shallower lapse rates occur during drier conditions.

d. Seasonal–synoptic variations

Synoptic types appear to impact T_{max} lapse rates for different seasons similarly (Fig. 8a). For example, dry tropical and transition weather types consistently produce the steepest mean T_{max} lapse rate for all seasons, except June–August. Dry polar and moist polar conditions consistently produce the shallowest mean lapse rates. This pattern is similar to that shown in the box plots for the grouping by synoptic type alone (Fig. 7a).

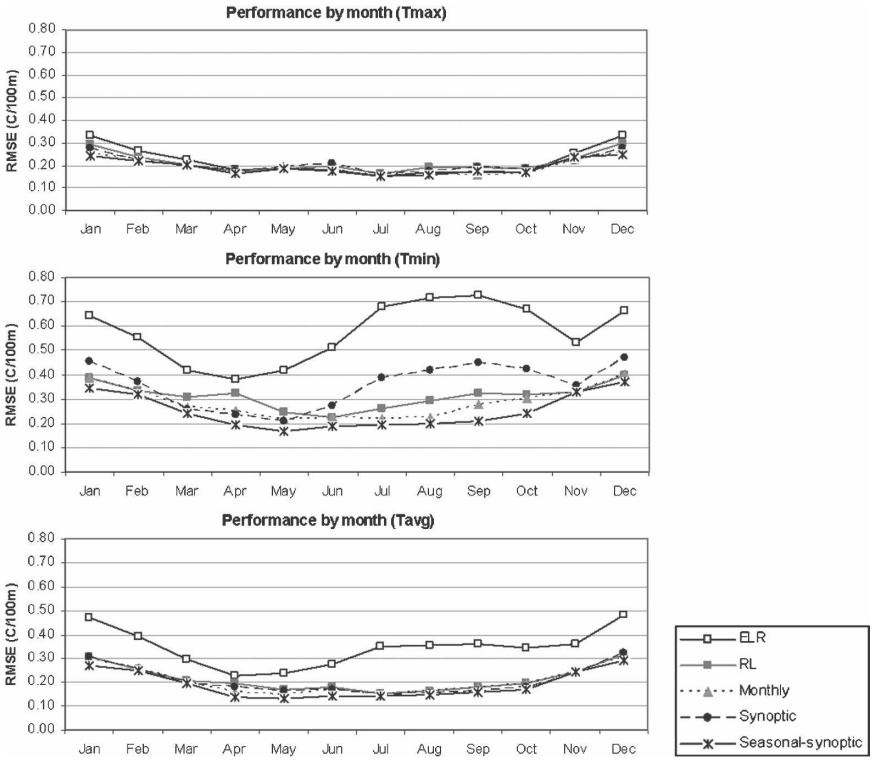

FIG. 9. Cross-validation results for (a) T_{max}, (b) T_{min}, and (c) T_{avg} lapse rates showing how well various group means predict the actual daily lapse rate. ELR represents the average atmospheric constant lapse rate and RL represents a regional lapse rate (long-term average) computed for the study area.

The box plots in Fig. 8b indicate that, like with T_{max}, the impact of synoptic types on T_{min} lapse rates is similar for different seasons. Drier conditions (DM, DP, and DT) consistently produce shallower mean lapse rates than wetter conditions (MM, MP) for all seasons, except December–February. Cold air masses, whether dry polar or moist polar, produce the shallowest mean lapse rates during December–February. This is consistent with the expectation that cold air may invert basin temperatures for an extended period of time during the winter. In the Boise study area, there are times in midwinter that deep inversions setup and only the highest mountains extend above the inversion. When this pattern sets up, low clouds and temperatures below freezing persist in the valleys, while mountain tops are sunny with above-freezing temperatures (J. Breidenbach 2006, personal communication). Such conditions may last for days and are likely the cause of the extreme extent of the box plots seen during polar conditions (DP, MP) in December–February.

e. Cross-validation results

Cross-validation results are plotted in Fig. 9. The plot of performance for T_{max} (Fig. 9a) indicates that the average ELR, RL, monthly, synoptic, and seasonal–synoptic lapse rates all perform similarly. However, small differences do occur in winter with seasonal–synoptic mean lapse rates performing best and the average atmospheric lapse rate performing worst. A seasonal trend exists in the performance of each lapse rate grouping. Performance is best in summer and worst in winter.

RMSEs in Fig. 9b show that T_{min} lapse rates are more difficult to predict than T_{max} lapse rates in all months. Performance using the ELR is drastically poorer than RL and monthly lapse rate performance. ELR performance is particularly poor from July to October. Regional and monthly rates perform comparably in winter, but monthly lapse rates perform better in spring and summer.

For the area evaluated in this study, monthly, synoptic, and seasonal–synoptic lapse rates appear to perform similarly (Fig. 9c). Annual average RMSE performance for T_{avg} was 0.21, 0.21, and 0.20°C (100 m)$^{-1}$, respectively. Surprisingly, overall the regional lapse rate performs nearly as well [0.22°C (100 m)$^{-1}$]. This is an artifact of using the mean as a predictor—it can perform no better than the standard deviation of each

TABLE 2. Recommended lapse rate values to use for different months. Although the values are specific to the study area, the general pattern should be similar elsewhere. Triangles indicate that the value is not significantly different than the regional lapse rate; asterisks indicate that the value is not significantly different than the average environmental lapse rate constant.

Month	T_{max} [°C (100 m)$^{-1}$]	T_{min} [°C (100 m)$^{-1}$]	T_{avg} [°C (100 m)$^{-1}$]
Jan	−0.43	−0.16△	−0.28
Feb	−0.51	−0.21	−0.36△
Mar	−0.54	−0.33	−0.43
Apr	−0.61△	−0.36	−0.49
May	−0.63	−0.29	−0.46
Jun	−0.68	−0.19	−0.43
Jul	−0.66*	−0.01	−0.33
Aug	−0.70	0.03	−0.33
Sep	−0.70	0.03	−0.34
Oct	−0.68	−0.05	−0.36△
Nov	−0.53	−0.23	−0.38△
Dec	−0.43	−0.12△	−0.28

grouping. We hypothesized that grouped lapse rates (subsets of the population) would have significantly lower sample standard deviations than the population as a whole (i.e., all 5527 daily lapse rates). This did not occur consistently—some groups had standard deviations lower than the population while others were higher. For example, the variability of T_{avg} lapse rates remained high even for the most strict subset (seasonal–synoptic grouping), with standard deviations ranging from 0.14° to 0.34°C (100 m)$^{-1}$. In cases where the within-group variation remains high, the subset mean will perform no better than the population mean. Nevertheless, the plots of performance (Fig. 9) identify time periods when different groupings are advantageous over the others. This is significant in terms of application because it indicates that the relevance and efficiency of the ELR and RL depends on the season and temperature variable (T_{max}, T_{min}, or T_{avg}) for which it is being used.

f. Recommended lapse rates

Since the cross-validation results indicated that monthly, synoptic, and seasonal–synoptic lapse rates all perform similarly, monthly groupings are recommended as a reasonable compromise between performance and ease of implementation. Synoptic and seasonal–synoptic groupings are considerably more difficult to develop than monthly groupings, and the SSC2 classification is not available for all areas. The recommended lapse rate values to use for different months are provided in Table 2. These lapse rates are specific to the study area and should be used with caution elsewhere, although the general pattern is thought to be relevant to basins in the Pacific Northwest of similar spatial scale (10 000 km^2). Applications of lapse rates should attempt to simulate these general seasonal patterns.

5. Summary

In this study, daily surface air temperature lapse rates were quantified at a spatial scale (10 000 km^2) that has not been evaluated thoroughly in other literature. Previous studies showed that over large temporal and spatial scales the lapse rate approximates the average environmental lapse rate constant (Barry 1992; Dodson and Marks 1997). Our study indicates that there are statistically significant variations from the environmental lapse rate constant during different times of year and synoptic conditions. Additionally, cross-validation results indicate that the ELR is solely applicable to maximum temperature—it often grossly overestimates minimum and average temperature lapse rates. Regional lapse rates (long-term mean of the daily values) perform better than the environmental lapse rate for T_{min} and T_{avg}, although for some months rates can be predicted more accurately by using monthly lapse rates.

The results of this study suggest that temporal variability in daily lapse rates can be taken into account to some degree by computing monthly averages. Synoptic and seasonal–synoptic groupings are also effective, but are considerably more cumbersome to implement than monthly. The Spatial Synoptic Classification system (SSC2) we used is only readily available for a limited number of stations (i.e., stations with long periods of records to guide the classification). Lapse rates computed for different months, synoptic types, and seasonal–synoptic categories all perform similarly; therefore, monthly lapse rates were chosen as a practical combination of effective performance and ease of implementation. The recommended lapse rates shown in Table 2 are specific to our study and may be helpful to local forecasters in Idaho who could, for example, use the information to assist efforts to produce a more realistic graphical temperature forecast (e.g., National Weather Service's National Digital Forecast Database). Monthly lapse rates in other study areas may be significantly different, but the methods used to obtain the recommended values are transferable to other study areas and are efficient to implement if meteorological station observations are available. Results also suggest that if observations are not available in the area of interest, then the ELR may be adequate for maximum air temperature and a regional lapse rate computed from a collection of the nearest observations may suffice for

average and minimum temperature (similar implications are made by Harlow et al. 2004). However, the major advantage described herein is that local, monthly lapse rates will perform with more consistency (i.e., smaller error for short time periods).

A better approach than lapse rates to distributing surface air temperature may be to use geostatistical spatial interpolation techniques, such as detrended ordinary kriging (Garen et al. 1994). However, one should be cautious about immediately accepting the more complex, spatially explicit methods as "better," because the computational intensity associated with these methods may outweigh the improvements brought to the model of interest. For example, semidistributed models, such as the Snowmelt Runoff Model, require mean areal temperature for zones rather than distributed values. The effect of averaging may supplant the benefits of a finer spatial resolution (i.e., fully distributed approach). A temperature interpolation method that simplistically considers spatial and temporal variability, such as the approach described herein, may perform comparably similar without the added computational time and effort. Trade-offs between performance and complexity should be investigated.

Acknowledgments. This research was funded by the Pacific Northwest Regional Collaboratory as part of Raytheon Corporation's Synergy project, funded by NASA through NAS5-03098, Task No. 110. Partial support was also provided by the NSF-Idaho EPSCoR program under Award Number EPS-0447689. The data for this project were provided by the Natural Resources Conservation Service and the National Weather Service. We thank Ron Abramovich (NRCS) and Jay Breidenbach (NWS) for helpful discussions, and Dr. Scott Sheridan provided the Spatial Synoptic Classification system and assistance in classifying weather types. Author Blandford thanks Dr. Stanley Miller for his review of the master's thesis that preceded this article. We also express our appreciation for the three anonymous reviewers whose comments improved the quality of this manuscript.

REFERENCES

Barry, R. G., 1992: *Mountain Weather and Climate.* 2nd ed. Routledge, 402 pp.

——, and R. J. Chorley, 1987: *Atmosphere, Weather, and Climate.* 5th ed. Methuen, 460 pp.

Bibby, J. S., H. A. Douglas, A. J. Thomasson, and J. S. Robertson, 1982: Land capability classification for agriculture. The Macaulay Institute for Soil Research, 75 pp.

Blöschl, G., 1991: The influence of uncertainty in air temperature and albedo on snowmelt. *Nord. Hydrol.,* **22,** 95–108.

Clements, C. B., C. D. Whiteman, and J. D. Horel, 2003: Cold-air-pool structure and evolution in a mountain basin: Peter Sinks, Utah. *J. Appl. Meteor.,* **42,** 752–768.

De Scally, F. A., 1997: Deriving lapse rates of slope air temperature for meltwater runoff modeling in subtropical mountains: An example from the Punjab Himalaya, Pakistan. *Mt. Res. Dev.,* **17,** 353–362.

Dodson, R., and D. Marks, 1997: Daily air temperature interpolated at high spatial resolution over a large mountainous region. *Climate Res.,* **8,** 1–20.

Ferguson, R. I., 1999: Snowmelt runoff models. *Prog. Phys. Geogr.,* **32,** 205–227.

Garen, D. C., G. L. Johnson, and C. L. Hanson, 1994: Mean areal precipitation for daily hydrologic modeling in mountainous regions. *Water Resour. Bull.,* **30,** 481–491.

Glahn, H. R., and D. P. Ruth, 2003: The new digital forecast database of the National Weather Service. *Bull. Amer. Meteor. Soc.,* **84,** 195–201.

Gustavsson, T., M. Karlsson, J. Bogren, and S. Lindqvist, 1998: Development of temperature patterns during clear nights. *J. Appl. Meteor.,* **37,** 559–571.

Harding, R. J., 1979: Altitudinal gradients of temperature in the northern Pennines. *Weather,* **34,** 190–201.

Harlow, R. C., E. J. Burke, R. L. Scott, W. J. Shuttleworth, C. M. Brown, and J. R. Petti, 2004: Derivation of temperature lapse rates in semi-arid southeastern Arizona. *Hydrol. Earth Syst. Sci.,* **8,** 1179–1185.

Jones, P. D., M. Hulme, and K. R. Briffa, 1993: A comparison of Lamb circulation types with an objective classification derived from grid-point mean sea-level pressure data. *Int. J. Climatol.,* **13,** 655–663.

Kidson, J. W., 1994: An automated procedure for the identification of synoptic types applied to the New Zealand region. *Int. J. Climatol.,* **14,** 711–721.

Lamb, H. H., 1972: *British Isles Weather Types and a Register of the Daily Sequence of Weather Patterns, 1861–1971. Geophysical Memoir,* No. 116, HMSO Met Office, 85 pp.

Lechowicz, M. J., 1984: Why do temperate deciduous trees leaf out at different times? Adaptation and ecology of forest communities. *Amer. Nat.,* **124,** 821–842.

Mahrt, L., D. Vickers, R. Nakamura, M. R. Soler, J. L. Sun, S. Burns, and D. H. Lenschow, 2001: Shallow drainage flows. *Bound.-Layer Meteor.,* **101,** 243–260.

Martinec, J. A., and A. Rango, 1998: Snowmelt Runoff Model (SRM) user's manual. USDA-ARS Hydrology and Remote Sensing Laboratory, 84 pp.

Mayes, J. C., 1991: Regional airflow patterns in the British Isles. *Int. J. Climatol.,* **11,** 473–491.

McCutchan, M. H., 1983: Comparing temperature and humidity on a mountain slope and in the free air nearby. *Mon. Wea. Rev.,* **111,** 836–845.

Muller, R. A., 1977: A synoptic climatology for environmental baseline analysis: New Orleans. *J. Appl. Meteor.,* **16,** 20–33.

Peacock, J. M., 1975: Temperature and leaf growth in *Lolium perenne*. I. The thermal microclimate: Its measurement and relation to crop growth. *J. Appl. Ecol.,* **12,** 99–114.

Pepin, N., D. Benham, and K. Taylor, 1999: Modeling lapse rates in the maritime uplands of northern England: Implications for climate change. *Arct. Antarct. Alp. Res.,* **31,** 151–164.

——, M. Losleben, M. Hartman, and K. Chowanski, 2005: A comparison of SNOTEL and GHCN/CRU surface temperatures with free-air temperatures at high elevations in the western United States: Data compatibility and trends. *J. Climate,* **18,** 1967–1985.

Reek, T., S. R. Doty, and T. W. Owen, 1992: A deterministic approach to the validation of historical daily temperature and precipitation data from the cooperative network. *Bull. Amer. Meteor. Soc.,* **73,** 753–762.

Régnière, J., 1996: A generalized approach to landscape-wide seasonal forecasting with temperature-driven simulation models. *Environ. Entomol.,* **25,** 869–881.

——, and P. Bolstad, 1994: Statistical simulation of daily air temperature patterns in eastern North America to forecast seasonal events in pest management. *Environ. Entomol.,* **23,** 1368–1380.

Richard, C., and D. J. Gratton, 2001: The importance of the air temperature variable for the snowmelt runoff modelling using SRM. *Hydrol. Processes,* **15,** 3357–3370.

Richner, H., and P. D. Phillips, 1984: A comparison of temperatures from mountaintops and the free atmosphere—their diurnal variation and mean difference. *Mon. Wea. Rev.,* **112,** 1328–1340.

Rolland, C., 2003: Spatial and seasonal variations of air temperature lapse rates in alpine regions. *J. Climate,* **16,** 1032–1046.

Running, S. W., R. R. Nemani, and R. D. Hungerford, 1987: Extrapolation of synoptic meteorological data in mountainous terrain and its use for simulating forest evapotranspiration and photosynthesis. *Can. J. For. Res.,* **17,** 472–483.

Schwartz, M. D., 1991: An integrated approach to air mass classification in the north central United States. *Prof. Geogr.,* **43,** 77–91.

Sheridan, S. C., 2002: The redevelopment of a weather-type classification scheme for North America. *Int. J. Climatol.,* **22,** 51–68.

Singh, P., and V. P. Singh, 2001: *Snow and Glacier Hydrology*. Kluwer Academic, 742 pp.

Stahl, K., R. D. Moore, and I. G. McKendry, 2005: Lapse rates of climate variables for different atmospheric circulation conditions. Headwater 2005: Hydrology, Ecology and Water Resources in Headwaters. Preprints, *Sixth Int. Conf. on Headwater Control,* Bergen, Norway.

Stoutjesdijk, P., and J. J. Barkman, 1992: *Microclimate, Vegetation, and Fauna*. Opulus Press, 216 pp.

Tabony, R. C., 1985: The variation of surface temperature with altitude. *Meteor. Mag.,* **114,** 37–48.

Thornton, P. E., S. W. Running, and M. A. White, 1997: Generating surfaces of daily meteorological variables over large regions of complex terrain. *J. Hydrol.,* **190,** 214–251.

Whiteman, C. D., X. Bian, and S. Zhong, 1999: Wintertime evolution of the temperature inversion in the Colorado Plateau Basin. *J. Appl. Meteor.,* **38,** 1103–1117.

Wigmosta, M. S., L. W. Vail, and D. P. Lettenmaier, 1994: A distributed hydrology–vegetation model for complex terrain. *Water Resour. Res.,* **30,** 1665–1679.

Zuzel, J. F., and L. M. Cox, 1975: Relative importance of meteorological variables in snowmelt. *Water Resour. Res.,* **11,** 174–176.